Physica Medica (2011) **27**, 75–80

available at www.sciencedirect.com

ScienceDirect

journal homepage: http://intl.elsevierhealth.com/journals/ejmp

ORIGINAL PAPER

A simple analytical expression to calculate the backscatter factor for low energy X-ray beams

U. Chica [a,b], G. Flórez [c], M. Anguiano [a], A.M. Lallena [a,*]

[a] *Departamento de Física Atómica, Molecular y Nuclear, Universidad de Granada, E-18071 Granada, Spain*
[b] *Centro Javeriano de Oncología, Pontificia Universidad Javeriana, Carrera 7, No. 40-62, Bogotá D.C., Colombia*
[c] *Secondary Standard Dosimetry Laboratory, Bogotá D.C., Colombia*

Received 29 October 2009; received in revised form 19 January 2010; accepted 31 March 2010

KEYWORDS
Backscatter factor;
X-rays

Abstract A simple analytical expression aiming to calculate the backscatter factor used in dosimetry protocols to determine the absorbed dose in water for low energy X-rays beams is presented. This expression is based on the linear dependence of the backscatter factor with the generating potential, for fixed values of the half-value layer. The results of a recent work in which 74 X-ray beams with different spectroscopic characteristics, generated with the code XCOMP5R and transported with the Monte Carlo code PENELOPE have been used. The expression derived permits to calculate the backscatter factor within 5% accuracy. The predictive power of this expression has been tested for 20 X-ray beams generated with potentials from 50 to 250 kV, for which half-value layers and backscatter factors have been experimentally determined.

Introduction

The backscatter factor is essential in the dosimetry of low energy X-ray beams. Various codes of practice [1–5] suggest that the absorbed dose at the surface of a water phantom for these beams can be calculated as

$$D_W = M_U\, N_K\, B \left(\frac{\overline{\mu}_{en}}{\rho}\right)_{w,air}, \qquad (1)$$

where M_U is the free-in-air chamber reading corrected to standard pressure and temperature, N_K is the air-kerma calibration factor, B is the backscatter factor and $(\overline{\mu}_{en}/\rho)_{w,air}$ is the water-to-air ratio of the mass energy absorption coefficients averaged over the primary photon spectrum in air. The backscatter factor accounts for the effect of the phantom scatter and is relevant in dosimetry and quality control in both radiodiagnosis [6–8] and radiotherapy [5,9,10].

The B factor has been studied from different points of view. It has been shown that it depends, mainly, on the X-ray spectrum, the corresponding half-value layer, HVL_1, and the field size [5,11]. Additional dependence on the

* Corresponding author. Tel.: +34 958 243216.
E-mail address: lallena@ugr.es (A.M. Lallena).

1120-1797/$ - see front matter © 2010 Associazione Italiana di Fisica Medica. Published by Elsevier Ltd. All rights reserved.
doi:10.1016/j.ejmp.2010.03.003

peak voltage of the tube [12], the anode angle [13], the source-to-surface distance [14], and the phantom thickness [15,16] and material [16–18] has been pointed out. Discrepancies between the different backscatter factors reported have been analyzed [13,19] and, to a large extent, have been explained.

The characterization of the low energy X-ray beams is based on the use of HVL_1 only as quality index. This causes an indetermination in the absorbed dose in water. The use of additional quality indexes should solve this problem. For example, HVL_1 and the tube potential, V, were considered to specify the f conversion factor for X-ray beam qualities [20]. Nevertheless, there is not yet enough information from experiments or theory on the calibration factors appearing in Eq. (1) with different quality indexes [11].

In a recent paper [21], the spectra of 74 X-ray beams, generated with the code XCOMP5R [22], were used as input for a series of Monte Carlo simulations, performed with the code PENELOPE [23] and conducted to calculate B and $(\overline{\mu}_{en}/\rho)_{w,air}$ for a field of 100 cm^2. The results of these simulations permitted us to estimate the uncertainties of D_W arising from the use of the HVL_1 only as quality index. Moreover, we showed that the use of HVL_1 and V could be a good option to fully characterize these beams.

In this paper we use the results from the Monte Carlo simulations above mentioned to study in detail the dependence of the B factor with HVL_1 and V. As a result, a simple expression which permits to calculate B as a function of these two quality indexes is obtained. In order to evaluate the predictive capacity of the expression found, it has been proven with comparison to 20 X-ray experimental beams for which the B factor and the HVL_1 were measured.

Materials and methods

The 74 X-ray beams were generated using the code XCOMP5R [22]. The particular characteristics of these beams can be found in [21]. They corresponded to tube potentials ranging from 20 to 150 kV and had HVL_1 values from 0.3 to 4.76 mm Al. The parameters were selected so that these beams could be gathered into 14 groups, each one comprising 5–7 beams characterized by the same HVL_1 value. A trial and error strategy was followed to select these beams. The various parameters used by XCOMP5R to generate the X-ray beams were changed until the desired HVL_1 values were obtained.

Using the spectra of these X-ray beams as input, we performed simulations with the Monte Carlo code PENELOPE [23] in which the backscatter factor B was calculated as the ratio of the water kerma at a point on the beam axis at the surface of a water phantom to the water kerma at the same point in absence of the phantom. Panel (a) in Fig. 1 shows a scheme of the geometry used in these simulations. We considered a point source irradiating a water phantom of $30 \times 30 \times 30$ cm^3, with a source-to-surface distance of 100 cm. Field sizes of 10×10 cm^2 in the phantom surface were considered. To score the kerma, we used a voxel of $2 \times 2 \times 0.2$ cm^3 centered in the beam axis, just inside the phantom.

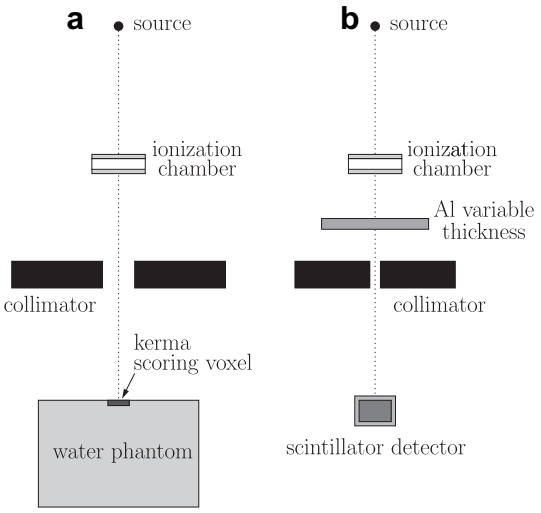

Figure 1 Scheme of the geometry used in the simulations and measurements done in this work to determine the backscatter factor (a) and the HVL_1 (b).

To check the procedure followed to obtain B, we compared the results found with four additional X-ray beams (see Table 2) with those quoted by Petoussi-Henss et al. [6]. As we can see, a nice agreement was found.

As it occurs for D_W (see [21]), B is not uniquely defined when HVL_1 is used as the only quality index; however, we found that B factors behave linearly with V for each HVL_1 value. Then we performed linear regressions to the calculated B factors using

$$B(HVL_1, V) = \delta_V(HVL_1) + m_V(HVL_1)V \quad (2)$$

These linear fits were done for each group of data characterized by the same value of HVL_1. In a second step, we assumed that the coefficients δ_V and m_V, obtained from these linear fits, depend linearly with HVL_1:

$$\delta_V(HVL_1) = a_\delta + b_\delta \cdot HVL_1, \quad (3)$$

$$m_V(HVL_1) = a_m + b_m \cdot HVL_1 \quad (4)$$

This two-step fit was checked calculating the quantity

$$\Delta = \frac{B_{approx} - B}{B}, \quad (5)$$

where B_{approx} is the B value predicted by using Eqs. (2)–(4).

In addition, we performed a series of experimental measurements in order to evaluate the predictive capacity of the approximate analytical expression deduced. We generated 20 X-ray beams with a PHILIPS MCN-321 (PHILIPS, Eindhoven, The Netherlands) three-phase device. Table 1 summarizes the accelerating potential and added filtration used for each one of these beams. In all cases a target angle of 22° was used.

For all these beams, attenuation curves in aluminium were measured following usual dosimetry protocols [5,11]. Panel (b) in Fig. 1 shows a scheme of the experimental setup. Measurements were done with a NE-110 plastic scintillator detector (Saint-Gobain, Newbury, U.S.A.) located at 100 cm from the target and centered at the

Table 1 Characteristics of the X-ray beams of the experiments presented in this work. The accelerating potential, V, the added filtration, HVL_1, and B are given.

Group	V	Filtration	HVL_1	B
	(kV)	(mm Al)	(mm Al)	
G1	62.5	3.0	2.34(6)	1.30(3)
	85.5	2.0	2.41(8)	1.31(3)
	120.5	1.0	2.37(7)	1.29(3)
	167.8	0.5	2.43(9)	1.28(3)
	236.5	0.2	2.40(10)	1.25(3)
G2	54.8	0.2	2.98(11)	1.28(3)
	65.8	0.5	3.03(8)	1.31(3)
	103.5	3.0	2.92(8)	1.32(3)
	160.7	2.0	3.12(10)	1.33(3)
	205.4	1.0	3.09(9)	1.34(3)
G3	54.7	8.0	3.49(10)	1.34(3)
	68.3	5.0	3.44(8)	1.37(3)
	99.2	3.0	3.63(10)	1.31(3)
	141.7	1.5	3.52(12)	1.33(3)
	209.1	0.5	3.44(12)	1.29(3)
G4	69.2	9.0	4.78(14)	1.39(3)
	86.8	7.0	4.96(15)	1.37(3)
	156.3	2.0	4.69(9)	1.35(3)
	203.5	0.9	4.81(11)	1.32(3)
	249.1	0.3	4.90(14)	1.30(3)

beam axis. An effective field with a radius of 2.5 cm was fixed by placing a circular collimator made of lead with a thickness of 5 mm and a diameter of 10 mm, at 80 cm in front of the detector. The Al foils with different thicknesses were located at 82 cm from the detector.

From the attenuation curves measured, the corresponding HVL_1 values were determined as described in previous works [21,24]. These values are given in the third column of Table 1. As we can see, the beams are gathered in such a way that those in a given set have a similar HVL_1 value.

A scheme of the experimental setup used to measure the backscatter factors is shown in panel (a) of Fig. 1. A WP34 (IBA Dosimetry GmbH, Schwarzenbruck, Germany) water phantom located at 100 cm downstream from the target was used. A circular radiation field with a radius of 5.6 cm at the phantom surface was fixed using a 4 mm thick lead collimator with a diameter of 2 cm, located at 17.9 cm above the phantom surface. Measurements were done with an ionization chamber PTW 30013 (PTW, Freiburg, Germany) situated just inside the phantom, as indicated by the kerma scoring voxel. The B values obtained as the ratio of the measurements done with and without the phantom are shown in Table 1 (fourth column).

Table 2 Comparison of our results for B, for a circular field of 100 cm^2, with those obtained by Petoussi-Henss et al. [6].

V	Filtration	HVL_1	B	
(kV)	[mm]	[mm Al]	This work	Petoussi-Henss et al.
70	2.5 Al	2.41	1.29(2)	1.30
80	3.0 Al	3.04	1.32(2)	1.34
90	3.0 Al	3.45	1.35(2)	1.35
120	3.0 Al	4.73	1.36(2)	1.37

In all the experiments carried out, the fluctuations in the dose rate were measured with an ionization chamber PTW NH30-360 (PTW, Freiburg, Germany) situated at 16 cm from the tube. They were below 0.2%.

The error in the measurements was evaluated from the uncertainties associated to the various magnitudes or procedures according to TRS-398 [11] and ISO [25]. The calibration factor of the secondary standard (1.0%), its long-range stability (0.2%), dosimeter reading relative to timer (0.1%), the establishment of the reference conditions (1%) and the beam energy dependence correction (1%) were considered. The total uncertainty was estimated to be $\sim$1.7%.

To check the capability of the model proposed, the experimental B values have been compared with the predictions of the empirical approximation found.

To finish we note that throughout the text, as well as in figures and tables, the uncertainties are given at 1σ level. On the other hand, when they are explicitly written, they are given as a number between parentheses (e.g., 2.37(7) means 2.37 ± 0.07).

Results and discussion

Fig. 2 shows (open squares) the B factors obtained from the Monte Carlo simulations for the 74 beams considered, as a function of V. The data have been plotted for the 14 different groups in which these beams were gathered. The HVL_1 value of each group is quoted in each panel. As anticipated, one can see that B depends linearly on V, for fixed HVL_1, in all cases. For each group of data and using Eq. (2), we performed the corresponding linear fits, which have been also plotted in each panel with solid lines.

It is worth stating that this is a noteworthy result. To our knowledge, it is the first time this behaviour of B versus HVL_1 and V is pointed out. On the other hand, and as we will see below, this opens the possibility of evaluating B in a unique form and avoiding the indetermination problem linked to the use of HVL_1 as the only quality index.

It is obvious that the coefficients δ_V and m_V, obtained after the linear regressions mentioned above, depend on HVL_1. The next step is then to parameterize this dependence. In Fig. 3 we have plotted these coefficients as a function of HVL_1. As we can see, different functions could be fitted to these values. However, in order to have the simpler expression, we have assumed that both coefficients depend linearly with HVL_1, as given by Eqs. (3) and (4). The results of the corresponding linear fits, which are shown with solid lines in Fig. 3, are

$$\delta_V(\mathrm{HVL}_1) = 1.03(2) + 0.098(7)\mathrm{HVL}_1,$$

$$m_V(\mathrm{HVL}_1) = 0.0011(1) - 0.00040(5)\mathrm{HVL}_1, \quad (6)$$

where HVL_1 is given in mm of Al and m_V is in $(\mathrm{kV})^{-1}$.

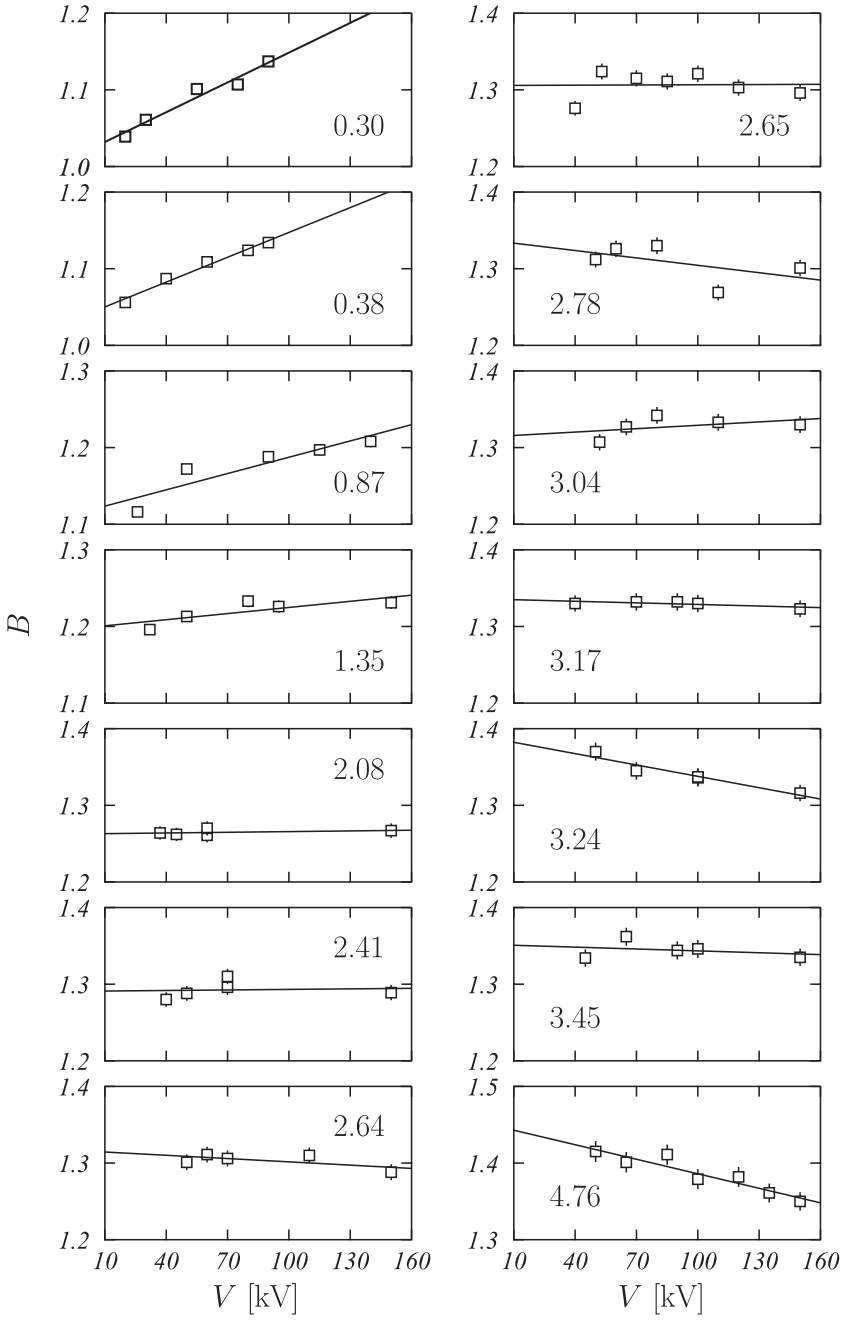

Figure 2 *B* versus *V* for the X-ray beams studied in this work (open squares). Solid lines give the corresponding linear fits. HVL_1 (in mm of Al) is given in each panel.

Eqs. (2)—(4), with the values shown in (6), provide, for the first time, a simple analytical expression to calculate the backscatter factor for low energy X-ray beams. This expression takes into account implicitly the linear dependence on *V* of the backscatter factor *B*, for fixed HVL_1, that we have found.

On other hand, and as it is well known [11], dosimeters used in clinical practice are not calibrated with the same combinations of *V* and HVL_1 as those of the user clinical beams. The expression here proposed should be an simple alternative to the interpolation needed in those cases.

To check the goodness of the fit performed, we calculated Δ, as defined in Eq. (5). The results are plotted in Fig. 4. They are within 5% in all cases and, except in a few cases of the first two groups and the last one, $\Delta = 0$ is compatible with the fit at 1σ level, which is the uncertainty plotted.

To validate the expression proposed, we have calculated approximated *B* values for the 20 experimental beams described above and we have compared them with those measured in our experiment in Fig. 5. Therein the gray bands indicate the uncertainty corresponding to the experimental values, while open squares represent the

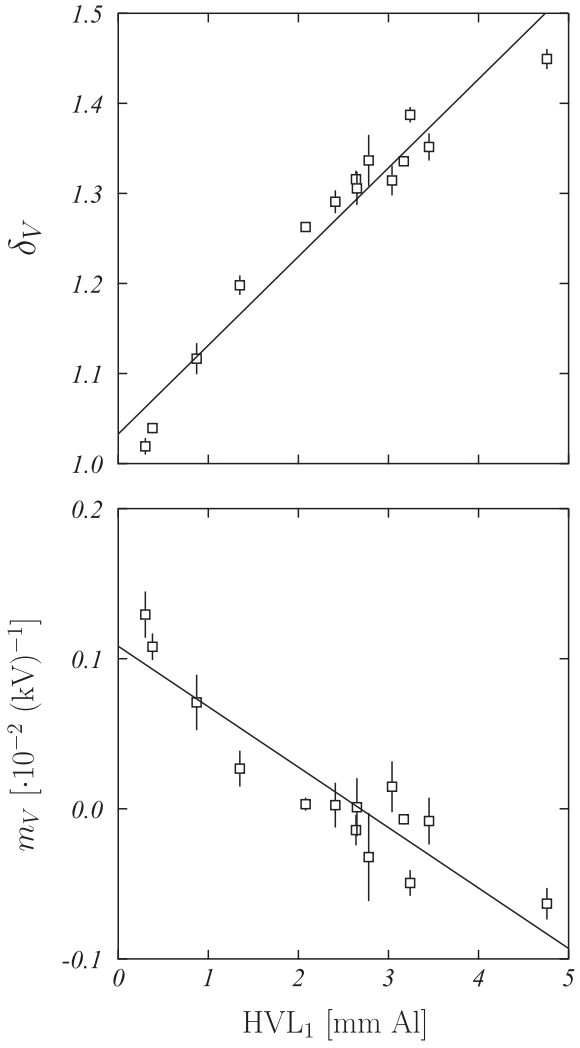

Figure 3 δ_V and m_V as a function of HVL$_1$. Solid lines are the results from linear fits to the data.

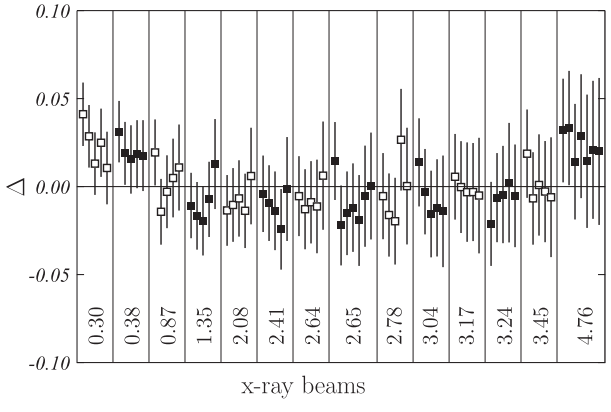

Figure 4 Relative differences Δ, as given by equation (5), for all the X-ray beams considered in this work. The values of HVL$_1$ for each group of beams are shown in mm of Al. The results corresponding to beams with a given HVL$_1$ value have been plotted contiguously and with the same symbol.

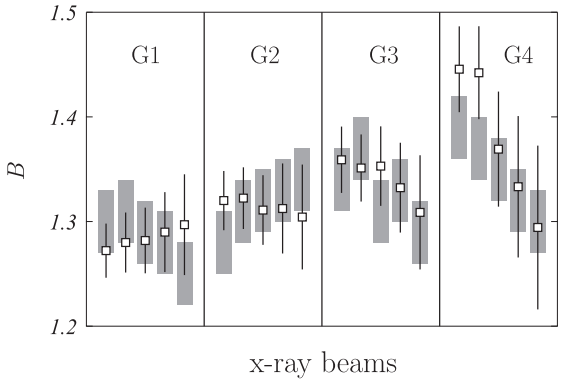

Figure 5 Comparison between the *B* values measured for the experimental 20 X-ray beams studied in this work (gray bands) and the approximated values obtained for the same beams with Eqs. (2) and (6) (open squares). The beams are grouped as in Table 1 and the plotting order is the same as in this table.

approximated ones. In all the cases the results are compatible at 1σ level (which is the uncertainty plotted). The largest relative difference (∼5.3%) corresponds to the second beam of the last group. This gives an idea of the maximum uncertainty in the *B* factors calculated with our approximation.

Conclusions

The backscatter factors calculated for 74 X-ray beams of low energy have been used to study how they depend on both HVL$_1$ and *V*. It has been shown that *B* depends linearly with *V* for fixed HVL$_1$, a behaviour that has not been pointed out before. Exploiting this dependence, we have obtained a simple analytical expression to calculate these factors using both HVL$_1$ and *V*. This expression, which comes from a double linear regression, has been tested using 20 experimental beams. We have found that the *B* factors obtained with the approximate expression reproduce the experimental values within 5%. It is worth noting that the only indexes needed are the HVL$_1$ and the tube potential, *V*, which are currently well known in practice.

Acknowledgements

This work has been partially supported by the Spanish Ministerio de Ciencia e Innovación under contract FPA2009-14091-C02-02 and by the Junta de Andalucía (FQM0220).

References

[1] Klevenhagen SC, Auckett RJ, Harrison RM, Moretti C, Nahum AE, Rosser KE. The IPEMB code of practice for the determination of absorbed dose for X-rays below 300 kV generating potential (0.035 mm Al-4 mm Cu HVL; 10—300 kV generating potential). Phys Med Biol 1996;41:2605—25.

[2] Deutsch Institüt für Normung (DIN). Klinische dosimetrie: anwendung von Röntgenstraheln mit Röhrenspanungen von 100 bis 400 kV in der Strahlentherapie (DIN6809-5). Berlin: DIN; 1996.

[3] Nederlandse Commissie voor Stralingsdosimetrie (NCS). Dosimetry for low and medium energy X-rays: a code of practice in radiotherapy and radiobiology. NCS Report 10. Delft: NCS; 1997.
[4] International Atomic Energy Agency (IAEA). Absorbed dose determination in photon and electron beams: an international code of practice. IAEA Technical Reports Series 277. Vienna: IAEA; 1987.
[5] Ma C-M, Coffey C, DeWerd L, Liu C, Nath R, Seltzer S, et al. AAPM protocol for 40—300 kV X-ray beam dosimetry in radiotherapy and radiobiology. Med Phys 2001;28:868—93.
[6] Petoussi-Henss N, Zankl M, Drexler G, Panzer W, Regulla D. Calculation of backscatter factors for diagnostic radiology using Monte Carlo methods. Phys Med Biol 1998;43:2237—50.
[7] Kramer R, Drexler G, Petoussi-Henss N, Zankl M, Regulla D, Panzer W. Backscatter factors for mammography calculated with Monte Carlo methods. Phys Med Biol 2001;46:771—81.
[8] Rosado PHG, Nogueira MS, Genezini F, Vilela EC. Measurement of conversion coefficients between free in air kerma and personal dose equivalent for diagnostic X-ray beams. Radiat Meas 2008;43:968—71.
[9] Harrison RM, Walker C, Aukett RJ. Measurement of backscatter factors for low energy radiotherapy (0.1—2.0 mm Al HVL) using thermoluminescence dosimetry. Phys Med Biol 1990;35:1247—54.
[10] Grosswendt B. Dependence of the photon backscatter factor for water on irradiation field size and source-to-phantom distances between 1.5 and 10 cm. Phys Med Biol 1993;38: 305—10.
[11] International Atomic Energy Agency (IAEA). Absorbed dose determination in external beam radiotherapy. IAEA Technical Reports Series 398. Vienna: IAEA; 2000.
[12] Harrison RM. Backscatter factors for diagnostic radiology (1—4 mm Al HVL). Phys Med Biol 1982;27:1465—74.
[13] Carlsson C. Differences in reported backscatter factors for low-energy X-rays: a literature study. Phys Med Biol 1993;38: 521—31.
[14] Grosswendt B. Dependence of the photon backscatter factor for water on source-to-phantom distance and irradiation field size. Phys Med Biol 1990;35:1233—45.
[15] Klevenhagen SC. The build-up of backscatter in the energy range 1 mm Al to 8 mm Al HVT. Phys Med Biol 1982;27:1035—43.
[16] Stanton L, Bratelli SD, Day LJ. Measurements of diagnostic X-ray backscatter by a novel ion chamber method. Med Phys 1982;9:121—30.
[17] Grosswendt B. Backscatter factors for X-rays generated at voltages between 10 and 100 kV. Phys Med Biol 1984;29: 579—91.
[18] Ma C-M, Seuntjens J. Mass—energy absorption coefficient and backscatter factor ratios for kilovoltage X-ray beams. Phys Med Biol 1999;44:131—43.
[19] Peixoto J, Andreo P. Determination of absorbed dose to water in reference conditions for radiotherapy kilovoltage X-rays between 10 and 300 kV: a comparison of the data in the IAEA, IPEMB, DIN and NCS dosimetry protocols. Phys Med Biol 2000; 45:563—75.
[20] Seuntjens J, Thierens H, Van der Plaetsen A, Segaert O. Conversion factor f for X-ray beam qualities, specified by peak tube potential and HVL value. Phys Med Biol 1987;32: 595—603.
[21] Chica U, Anguiano M, Lallena AM. Study of the formalism used to determine the absorbed dose for low-energy X-ray beams. Phys Med Biol 2008;53:6963—77.
[22] Nowotny R, Höfer A. Ein Program für die Berechunung von diagnostischen Röntgenspektren. Fortschr Röntgenstr 1985; 142:685—9.
[23] Salvat F, Fernández-Varea JM, Sempau J. PENELOPE-A code system for Monte Carlo simulation of electron and photon transport. Paris: Nuclear Energy Agency; 2006.
[24] Chica U, Anguiano M, Lallena AM. Benchmark of PENELOPE for low and medium energy X-rays. Physica Medica Eur J Med Phys 2009;25:51—7.
[25] International Organization for Standardization (ISO). Guide to the expression of uncertainty in measurement. Geneva: ISO; 1995.